Journal of Environment & Biotechnology Research
VINANIE PUBLISHERS
www.vinanie.com/jebr

Jackfruit seed as a sustainable adsorbent for the removal of Rhodamine B dye

Muhammad Raziq Rahimi Kooh,* Muhammad Khairud Dahri, Linda B. L. Lim

Chemical Sciences Programme, Universiti Brunei Darussalam, Jalan Tungku Link, Pengkalan Gadong, Bandar Seri Begawan, BE 1410, Brunei Darussalam

ORIGINAL RESEARCH ARTICLE

ABSTRACT

Jackfruit seed (JS) was used in this study to investigate its potential as an adsorbent to remove rhodamine B (RB) dye from aqueous solution. Surface morphology and functional group analyses were carried out to characterise the adsorbent. Experimental parameters such as contact time, temperature, adsorbent dosage, dye concentration, medium pH and ionic strength were studied to explore their effects on the adsorption of RB dye onto the adsorbent. Thermodynamics, kinetics and isotherm models were applied on the experimental data in order to further understand the adsorption process and mechanism. The Langmuir and Sips models best described the adsorption process with predicted maximum adsorption capacity of 26.4 and 37.9 mg/g, respectively. The pseudo-second-order model best fitted the kinetics model and thermodynamics studies revealed adsorption process is endothermic.

KEYWORDS

adsorption; *Artocarpus heterophyllus*; electrostatic interaction; hydrophobic-hydrophobic interaction; Rhodamine B dye

1. INTRODUCTION

The textile industry generally consume large amount of freshwater and the waste subsequently generated from the dyeing section was estimated to be up to 15% of the total wastes (Kant, 2012). Most of the freshwater pollution is mainly caused by textile and agriculture industries (Kant, 2012). This may be due to the chemical stability of the synthetic dyes which are resistant to photo-degradation, chemical-degradation and thermal-degradation. Dye wastewater has become a great concern for many countries. In some countries where stringent laws although are in place but not strictly enforced, and this has led to pollution of many freshwater resources and causing harm to aquatic flora and fauna, as well as whoever are using the polluted freshwater for domestic purposes (Awomeso et al., 2010; Ahmed et al., 2012; Bello et al., 2013).

There are many remediation methods for dye wastewater treatment. Some of these methods include adsorption, addition of oxidising or reducing agents, electro-degradation, catalytic degradation using Fenton's reagent, microbial degradation as well as membrane filtration (Forgacs et al., 2004). Their advantages and disadvantages were widely discussed in the literature. Among all the dye wastewater remediation technologies, adsorption itself is the most researched method during the last decade (Wang et al., 2011). Adsorption can be applied and easily adopted by responsible factories due to its simple remediation procedures (Kooh et al., 2015b) and the scalability of dye wastewater treatment can also be easily adjusted. The main constraint of adsorption method is the cost of dye wastewater treatment and the cost depends on the type of adsorbent as well as its removal efficiency. Low-cost adsorbents may include those materials that are in abundant such as Casuarina tree (Dahri et al., 2015), fungus (Idowu et al., 2016), seaweed (Vijayaraghavan, 2015) and freshwater weed (Kooh et al., 2015a), soil materials (Chieng et al., 2014) and those derived from

Corresponding author: **M.R.R. Kooh**
Tel: +673 8658876
Fax: +673 2461502
E. mail: chernyuan@hotmail.com

Received: 13-05-2016
Revised: 28-05-2016
Accepted: 20-06-2016
Available online: 01-07-2016

agriculture (Lim et al., 2014) or industrial wastes such as soya bean waste (Kooh et al., 2016b) and sawdust (Anagnostopoulos et al., 2015). Adsorbents with higher cost may include those materials that involved chemical treatment (Kooh et al., 2016c) or thermal treatment such as activated carbon (Kavitha, 2016) and any carbonaceous materials (Hameed et al., 2007).

The main aim of this research is to investigate the potential of jackfruit seeds (JS) as low-cost adsorbent to remediate rhodamine B (RB) dye wastewater. Jackfruit (*Artocarpus heterophyllus*) tree is an evergreen tree that is found worldwide which include the South-East Asian nations, India, Florida, Central and Eastern African nations, Caribbean islands, Australia and most of the Pacific islands (Prakash et al., 2009). The tree bears huge fruit with pungent fleshy yellow pulp and huge seeds. For most of the time, only the fleshy pulp is eaten while the seeds are considered as a by-products and are usually discarded which represented 8-15% of the total fruit weight (Madruga et al., 2014). The seeds are mainly consumed in the lower-income countries where the seeds can be roasted, boiled and steamed which produce aromatic and nutty taste. Locally, the seeds are usually diced and cook with curry, however they are not popular cuisines due to the texture of seed and bland taste. The bland taste may be due to its high starch content which is approximate 93 to 95% (Madruga et al., 2014). On the other hand, starch-containing materials were reported to be effective in dye removal where corn starch and wheat starch removed approximately 37 and 39% of acid blue 193, respectively (Blackburn, 2004), and these results indicate that JS may be a good candidate for dye removal. This research will increase the value of *Artocarpus heterophyllus*.

This study focuses on a hazardous xanthine dye, Rhodamine B (RB), which is widely used in paint, textiles, paper and leather industries (Santhi et al., 2014). It is a maroon coloured solid which dissolves in water to produce bright pink solution. Animal testing revealed that RB causes tumours and induces reproductive toxicity in rats, and it is also highly toxic to fish where LC50 of 83.9 mg/L for sheepshead minnow was reported (SIGMA-ALDRICH, 2014)

2. MATERIALS AND METHODS

2.1. Preparation of adsorbate

Rhodamine B (RB) (95% dye content, Mr 479.01 g/mol) was purchased from Sigma-Aldrich. RB stock solution at 500 mg/L was first prepared by dissolving the desired amount of solid in distilled water. Other concentrations were prepared by serial dilution.

2.2. Preparation of adsorbent

Jackfruits were bought from local markets and the rind, fleshy pulps and seeds were separated. The seeds were washed with distilled water, diced into small pieces and dried in oven at 70 ^{o}C. After drying, the diced seeds were pulverised using a blender and sieved to size less than 355 μm, and stored in desiccators until further use.

2.3. Characterisation of adsorbent

The adsorbents were characterised by functional group analysis, surface morphology analysis and determination of its point of zero charge. Functional group analysis was carried out using Fourier transform infrared (FTIR) spectroscopy using the KBr disc method. The KBr (Sigma-Aldrich, spectroscopy grade) was dried at 120 ^{o}C in an oven for 3 h prior to use in order to remove water. All FTIR spectra were obtained using a Shimadzu Model IR Prestige-21 spectrophotometer. Surface morphology analysis was carried out by using a Tescan Vega XMU scanning electron microscope (SEM) under vacuum and accelerating voltage of 30 kV, and the adsorbent particles were mounted on carbon conducting tape and gold-coated using SPI-MODULE™ Sputter Coater at plasma current 8 mA for 60 seconds. The point of zero charge (pH_{pzc}) of the adsorbent was determined by the salt addition method (Zehra et al., 2015). The pH of the 0.1 mol/L NaCl solution (20.0 mL) was adjusted using HNO_3 and NaOH to obtain initial pH ranged from 2.0 to 10.0. Adsorbent (0.04 g) was transferred and sealed with parafilm followed by 24 h agitation using a Stuart orbital shaker at agitation speed of 250 rpm. The final pH was measured using a Thermo-Scientific pH meter and the linear plot of pH difference, ΔpH (final pH - initial pH) vs initial pH, was used to determine the pH_{pzc}.

2.4. Batch adsorption procedure

The general procedure of carrying out the batch adsorption procedure is by adding 0.04 g of adsorbent to 20 mL dye solution in Erlenmeyer flasks with volume capacity of 150 mL, and agitates the solutions using a Stuart orbital shaker at agitation speed of 250 rpm for 2.5 h, unless otherwise stated. The concentration of dye of the filtrate after the agitation process was

determined using an UV–visible spectrophotometer (Shimadzu UV-1601PC) at a wavelength of 555 nm.

The adsorption capacity, q_e (mg/g), is the amount of dye adsorbed per gram of adsorbent at equilibrium, and the equation can be defined as:

$$q_e = \frac{(C_i - C_e)V}{m} \quad (1)$$

where C_i is the initial dye concentration (mg/L), C_e is the RB concentration in the filtrate at equilibrium (end) of the adsorption process (mg/L), V is the volume of RB used (L) and m is the mass of the adsorbent (g).

The % removal of dye was calculated by the following equation:

$$\%\ removal = \frac{(C_i - C_e) \times 100\%}{C_i} \quad (2)$$

A few parameters were investigated, which include the effects of pH (2 – 8), ionic strength (0 – 0.8 mol/L NaCl), contact time (5 – 240 min) and C_i (20 – 500 mg/L). One parameter was changed at a time while others were being kept constant.

The adsorption data were characterised using the Langmuir (1916), Freundlich (1906), Sips (1948) and Dubinin-Radushkevich (D-R) (Dubinin and Radushkevich, 1947) isotherm models, while the kinetics data were characterised using pseudo-first-order (Lagergren, 1898), pseudo-second-order (Ho and McKay, 1999) and Weber-Morris intraparticle diffusion models (Weber and Morris, 1963).

The value of the coefficient of determination, R^2, determines the best-fitting isotherm and kinetics models. Viable linear regression tools such as the Chi-square (χ^2) and sum of absolute error (EABS) were also used to reinforce the models that described the adsorption data. The equation of the error analyses are as follows:

$$\text{EABS: } \sum_{i=1}^{n} \left| q_{e(\exp)} - q_{e(cal)} \right| \quad (3)$$

$$\chi^2 : \sum_{i=1}^{n} \frac{(q_{e(\exp)} - q_{e(cal)})^2}{q_{e(\exp)}} \quad (4)$$

where $q_{e(exp)}$ is the experimental value while $q_{e(cal)}$ is the calculated value, n is the number of data points in the experiment and p is the number of parameters of the model.

2.5. Thermodynamics study

The Van't Hoff equation was applied to investigate the thermodynamics nature of the adsorption process. The range of temperature included in the thermodynamics studies was from 25 to 55 °C. The equations are expressed as:

$$\Delta G^0 = \Delta H^0 - T\Delta S^0 \quad (5)$$

$$\Delta G^0 = -RT \ln k \quad (6)$$

$$k = \frac{C_s}{C_e} \quad (7)$$

$$C_s = C_i - C_e \quad (8)$$

where T is the temperature in Kelvin (K), ΔG^o is the Gibbs' free energy, ΔS^o is the change in entropy, ΔH^o is the change in enthalpy, k is the distribution coefficient for adsorption, C_s is the amount of RB adsorbed by the adsorbent after equilibrium (mg/L), and R is the gas constant (8.314 J/mol K).

By substituting equation (5) into equation (6), the following equation is derived:

$$\ln k = \frac{\Delta S^o}{R} - \frac{\Delta H^o}{RT} \quad (9)$$

The ΔS^o and ΔH^o were calculated from the linear plot of ln k vs 1/T.

2.6. Regeneration experiments

The regeneration experiments involved two solvents (distilled water and 0.1 mol/L NaOH), and the detailed procedure was described in our previous work (Dahri et al., 2014). In general, spent adsorbent was prepared by agitating the unused adsorbent in 50 mg/L RB for 2 h. Distilled water washing was carried out by agitating spent adsorbent in 100 mL of distilled water several times at 30 min interval. The regenerated adsorbent was dried at 70 °C for 24 h. The basic washing was carried out by agitating the spent adsorbent in 0.1 mol/L NaOH for 30 min, followed by repeated washing with distilled water until the pH of the washed solution is near neutral. The regenerated adsorbent was then dried at 70 °C for 24 h. The regeneration experiments were repeated up to 3 cycles.

3. RESULTS AND DISCUSSION

3.1. Characterisations of adsorbent

Surface morphology analysis provides visual insights into the surface of the adsorbent at higher magnification. The SEM image of the adsorbent particle is as shown in Figure 1. It can be observed that the surface of JS is irregular, rough, and without any orderly pattern.

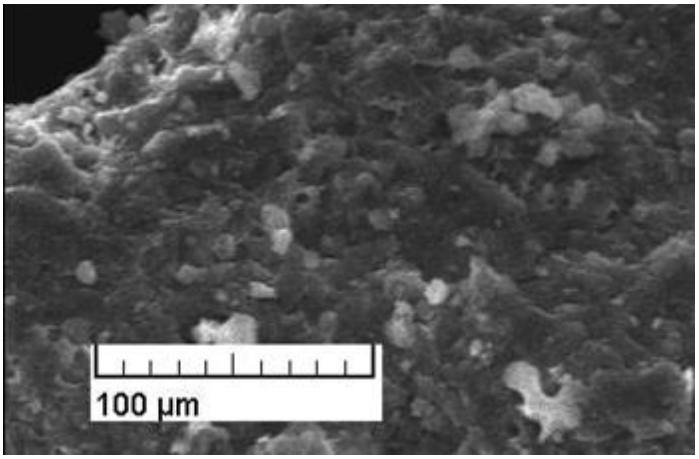

Figure 1. SEM image of an adsorbent particle at magnification of 400x.

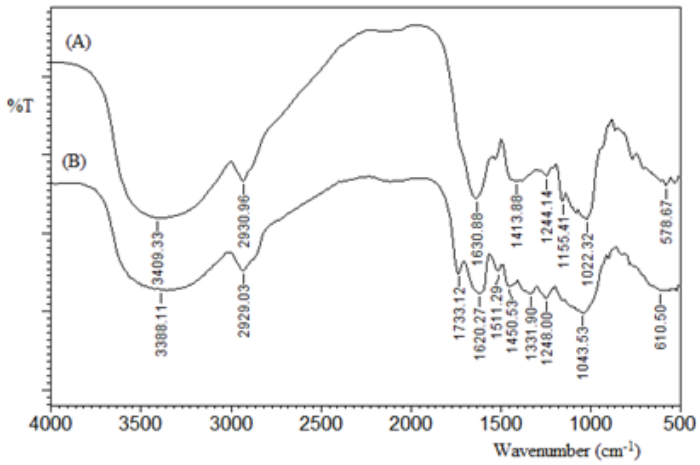

Figure 2. FTIR spectra of (A) JS and (B) JS-RB.

The FTIR spectra of the adsorbent, before and after RB treatment, are as shown in Figure 2. The FTIR spectrum of JS revealed the presence of O—H and amine groups (3409 cm^{-1}), C—H stretch (2930 cm^{-1}), N—H bending (1630 cm^{-1}), phenyl (1413 cm^{-1}) and C—O—C (1022 cm^{-1}). After dye treatment, it can be observed that there is a shift of bands for O—H and amine groups (3388 cm^{-1}), N—H bending (1620 cm^{-1}), phenyl (1450 cm^{-1}) and C—O—C (1048 cm^{-1}), indicating these groups may have interact with the RB dyes. The new band at 1331 cm^{-1} may be due to the C—N stretching for amide of RB which confirms the loading of the RB dye.

3.2. Point of zero charge and effects of pH and ionic strength

The effects of pH and ionic strength are important in the adsorption study as these parameters can influence the interactions between the adsorbate and adsorbent. It is established that the dye interacts with adsorbent particles by two main mechanisms: the electrostatic interaction and non-electrostatic interaction (Hu et al., 2013). Non-electrostatic interactions include both the hydrophobic-hydrophobic interaction and hydrogen bonding. Hydrophobic-hydrophobic interaction simply means the interaction between the non-polar groups of the dye molecule with the non-polar groups of the adsorbent surface.

The pH_{pzc} of JS was determined as 3.75, where the surface of the adsorbent particles has zero net charge. When the pH of the aqueous solution is higher than the pH_{pzc} value, then the net surface charge is predominantly negatively charged, while the opposite is true when pH of aqueous solution is lower than pH_{pzc}. The pH of the aqueous solution mainly affect the charge of the functional groups on the adsorbent surface therefore the pH of aqueous solution directly control the electrostatic interaction between the dye and the adsorbent. In Figure 3A, it can be observed that pH lower than pH_{pzc} resulted in decreased dye removal, while pH above pH_{pzc} resulted in slightly higher dye adsorption. This reduction of dye removal for solution pH < pH_{pzc} may be due to the surface of the adsorbent being predominantly positively charged leading to electrostatic repulsion of the positively-charged RB.

The general behaviour for the effect of ionic strength in the removal of RB by JS is shown in Figure 3B. The performance of an adsorbent can be affected by the present of salts in the water as electrostatic interaction and hydrophobic-hydrophobic interaction can be influenced by ionic strength (Hu et al., 2013). When the ionic strength is high enough, the electrostatic interaction can be totally suppressed due to competition betwen cations and the adsorbates for adsorption sites (Hu et al., 2013). The removal of 50 mg/L RB in the absence of salt was around 48% which decreased to 43% in the presence of 0.1 mol/L salts. Further increase in the salt concentration does not

significantly alter the dye removal whereby around 41% dye uptake was observed at salt concentration of 0.8 mol/L. Overall, changing the solution ionic strength did not significantly affect the performance of JS in removing RB and it can be said that electronic interaction did not play a major role in the adsorption process, while non-electrostatic interaction could be the dominant force between the adsorbent-absorbate interaction. This can be viewed as an advantage as JS can be used to remove RB in water with high salt content.

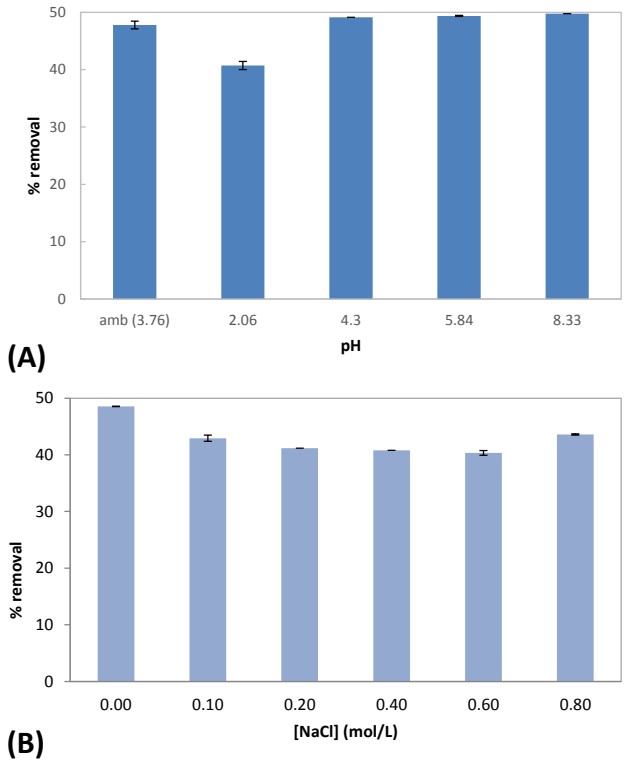

Figure 3. Effects of (A) pH and (B) ionic strength on the adsorption of RB using JS.

3.3. Effect of contact time and kinetics modelling

Contact time is a very useful parameter which can be used as an indication on how fast the adsorption reaches equilibrium. Figure 4A shows the effect of contact time on the adsorption of 50, 100 and 200 mg/L RB onto JS. It can be seen that all three concentrations displayed similar trend whereby the q_e value increased rapidly at the initial time up to 60 min, after which the adsorption increased only slightly and reached a plateau at 150 min. Generally as the dye-adsorbent mixture is agitated, the dye molecules will start to fill the surface active sites and these sites get saturated as the agitation continues, hence the q_e value started to reach a plateau. Through this study, it was determined that equilibrium was reached within 2.5 h.

In order to investigate the adsorption mechanism, three kinetics models namely pseudo-first-order (Lagergren, 1898), pseudo-second-order (Ho and McKay, 1999) and Weber-Morris intraparticle diffusion (Weber and Morris, 1963) were used to fit the experimental data of contact time. The linear expressions of the three models are shown as:

Pseudo-first-order:

$$log\ (q_e - q_t) = log\ q_{e(cal)} - k_1 \frac{t}{2.303} \quad (10)$$

Pseudo-second-order:

$$\frac{t}{q_t} = \frac{1}{q_{e(cal)}{}^2 k_2} + \frac{t}{q_e} \quad (11)$$

Weber-Morris intraparticle diffusion:

$$q_t = k_3\, t^{1/2} + C \quad (12)$$

where q_e is the adsorption capacity of the adsorbent at equilibrium (mg/g), q_t is the adsorption capacity (mg/g) at time t (min), $q_{e(cal)}$ is the calculated adsorption capacity (mg/g), k_1 is the pseudo-first-order rate constant (min^{-1}), k_2 is pseudo-second-order rate constant (g/ mg min), k_3 is the intraparticle diffusion rate constant (mg/g $min^{1/2}$) and C is the intercept.

The linear plots of $log(q_e-q_t)$ vs t, t/q_t vs t and q_t vs $t^{1/2}$ were constructed in order to calculate the parameters of the pseudo-first-order, pseudo-second-order and Weber-Morris intraparticle diffusion models, respectively. Table 1 summarises the parameters of the kinetics models. Comparing between the pseudo-first-order and pseudo-second-order, it can be seen that the coefficient of determination (R^2) value of the latter is higher (>0.98) for all the concentrations. This suggests the suitability of pseudo-second-order to describe the adsorption mechanism. This is further supported by the close agreements of equilibrium uptakes predicted by the pseudo-second-order with the experimental qe value ($q_{e(exp)}$) as well as the low χ^2 and EABS. Hence the rate of adsorption of RB followed a second-order rate law in terms of the availability of adsorption sites on the surface of JS rather than the amount of RB in the bulk solution (Liu, 2008).

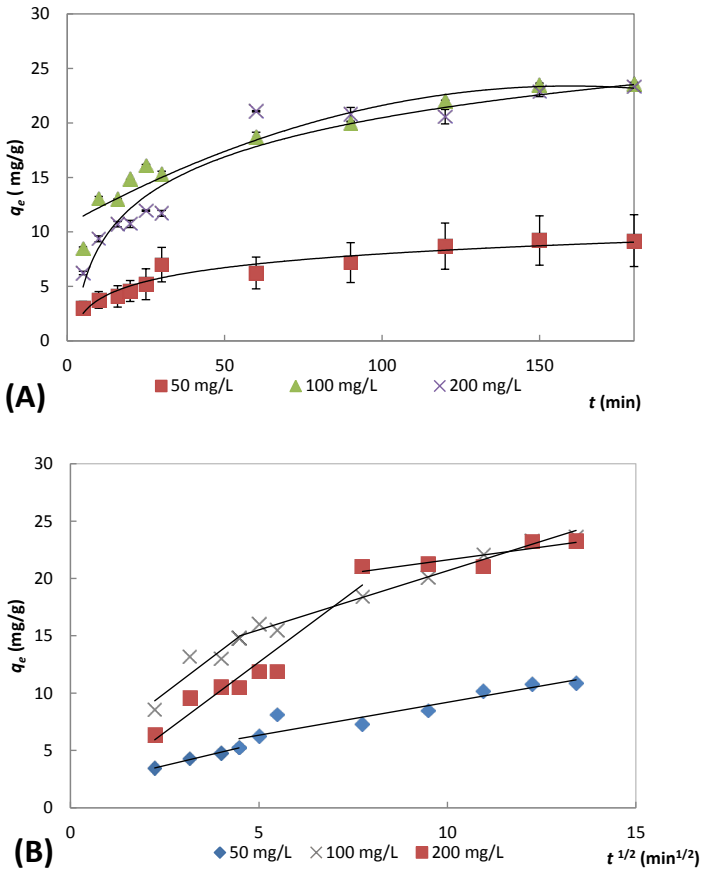

Figure 4. (A) Effect of contact time and (B) Weber-Morris intraparticle diffusion model's plots.

Unlike the previous two models, the Weber-Morris model can be used to investigate the diffusion mechanism that occurs during the adsorption process. Intraparticle diffusion is considered as the rate limiting step when the linear plot of Weber-Morris passes through the origin. In case of multi linear Weber-Morris plot is observed, the adsorption process is controlled by more than one mechanism. Generally, three phases can be found in the multi linear plot; 1) the fast initial phase which represent surface diffusion, 2) the intraparticle diffusion phase and 3) the equilibrium phase (Olu-Owolabi et al., 2014). However, only two phases were seen for the diffusion process as shown in Figure 4B, as the first phase is a fast process. As seen from Table 1 and Figure 4B, the plots did not pass through the origin and thus, intraparticle diffusion was not the rate limiting step and more than one mechanism could be involved. It is noted that the C values for all of the concentration were small which suggests that surface diffusion did not play major role as the rate limiting step (Olu-Owolabi et al., 2014).

Table 1. The kinetics parameters for the adsorption of RB by JS.

Pseudo-first-order			
C_i (mg/L)	50	100	200
$q_{e(cal)}$ (mg/g)	9.9	15.4	24.3
$q_{e(exp)}$ (mg/g)	10.9	23.7	23.3
k_1	0.027	0.021	0.033
R^2	0.846	0.939	0.834
χ^2	5	50	4
EABS	15	93	19
Pseudo-second-order			
$q_{e(cal)}$ (mg/g)	12.0	25.0	26.5
$q_{e(exp)}$ (mg/g)	10.9	23.7	23.3
k_2	0.0037	0.0027	0.0015
R^2	0.981	0.994	0.987
χ^2	8	12	17
EABS	19	39	41
Weber-Morris intraparticle diffusion			
C_i (mg/L)	50	100	200
k_3	0.781	2.493	2.452
C	1.732	3.753	0.438
R^2	0.991	0.837	0.919

3.4. Effect of initial dye concentration and adsorption isotherm analysis

The effect of initial dye concentration is shown in Figure 5 where the adsorption capacity increases as the dye concentration increases. This increase was only observed up to 300 mg/L and beyond this concentration there was no significant change in the q_e value. The initial increase was due to the concentration gradient which provided enough force to drive the mass transfer rate (Rehman et al., 2013) and as the adsorbent's active sites became saturated, the dye uptake did not increase any further.

The experimental data were fitted into the Langmuir, Freundlich, Sips and Dubinin-Radushkevich (D-R) models in order to investigate the adsorption process. The application of these isotherm models had been discussed in the literature (Foo and Hameed, 2010). The linear equations of the models are as follows:

Langmuir:

$$\frac{C_e}{q_e} = \frac{1}{K_L\, q_m} + \frac{C_e}{q_m} \quad (13)$$

Freundlich:

$$lnq_e = \frac{1}{n_F}\, lnC_e + lnK_F \quad (14)$$

Sips:

$$ln\left(\frac{q_e}{q_m - q_e}\right) = K_{LF} ln\, C_e + ln\, K_S \quad (15)$$

D-R:

$$\ln q_e = \ln q_m - K_{DR}[RT\left(1 + \frac{1}{C_e}\right)]^2 \quad (16)$$

where q_m (mg/g) is the maximum adsorption capacity, K_L (L/mg) is the Langmuir constant, K_F ((mg/g) (L/mg)$^{1/n_F}$) is the adsorption capacity of the adsorbent, n_F value (between 1 and 10) indicates favourability of the adsorption process, K_S (L/g) is Sips constant, K_{LF} is the exponent, K_{DR} (mol²/kJ²) is D-R constant, R (8.314 J/mol K) is the gas constant and T (K) is the absolute temperature and E (kJ/mol) is the mean free energy.

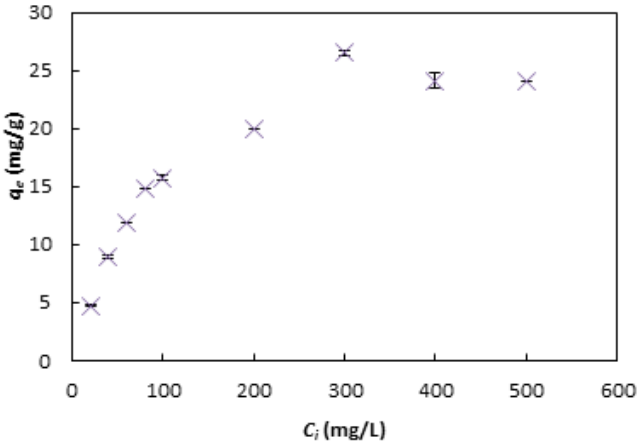

Figure 5. The effect of RB concentration on the adsorption of the dye onto JS.

The separation factor (R_L) of the Langmuir model (Weber and Chakravorti, 1974) can be used for determining the favourability of the adsorption process. The equation is as follows:

$$R_L = \frac{1}{(1 + K_L C_i)} \quad (17)$$

If the value of R_L is zero, more than 1, equal to 1, or between 0 and 1, this indicates the adsorption is irreversible, unfavourable, linear and favourable, respectively (McKay et al., 1982).

The adsorption process is predicted to be either physical or chemical in nature by estimating the mean free energy of adsorption, E (kJ/mol) where the equation is as follows:

$$E = \frac{1}{\sqrt{2k_{DR}}} \quad (18)$$

From Table 2, it can be seen that Sips has the highest R^2 value amongst the isotherm models while Langmuir has the smallest value for both error functions. Therefore, both the Sips and Langmuir can be used to describe the experimental data. It is noted that both the R_L and nF values showed that the adsorption of RB onto JS is favorable. The q_m of JS in the removal of RB is 24.6 mg/g which is higher than 22.4 mg/g as reported for *Acacia* leaf (Santhi et al., 2014). However the q_m was lower than water fern (72.2 mg/g) (Kooh et al., 2016d), *Casuarina equisetifolia* needles (82.3 mg/g) (Kooh et al., 2016a), and peat (85.5 mg/g) (Chieng et al., 2015).

Table 2. The calculated parameters of the Langmuir, Freundlich, Sips and Dubinin-Radushkevich.

Langmuir		Freundlich	
q_m (mg/g)	26.4	K_F((mg/g) (L/mg)$^{1/n_F}$)	3.071
K_L (L/mg)	0.030	n_F	2.701
R_L	0.1		
R^2	0.993	R^2	0.927
χ^2	0.6	χ^2	2.8
EABS	7.9	EABS	18.4
Dubinin-Radushkevich		Sips	
q_m (mg/g)	18.2	q_m (mg/g)	37.9
K_{DR} (mol²/kJ)	10.9	K_s (L/mg)	0.055
E (kJ/mol)	0.214	K_{LF}	1.635
R^2	0.705	R^2	0.997
χ^2	11.9	χ^2	0.9
EABS	37.1	EABS	10.0

3.5. Thermodynamics experiments

The thermodynamics experiments give useful insights on the thermal effect on the adsorption process. At

temperature of 25, 35, 45 and 55 °C, the % removal were 41.8, 48.5, 54.0 and 58.9%, respectively which showed that dye adsorption increased with temperature. Referring to Table 3, the value of ΔG° became more negative with the increase of temperature which indicated an increase in spontaneity of the adsorption process with the increase in temperature. The positive value of the ΔH° indicates that the adsorption process is endothermic in nature while the positive value of ΔS° indicates that the adsorption process resulted in the increase of randomness in the solid-liquid interface.

Table 3. Thermodynamics parameters of the JS-RB system.

T (°C)	Δ*G*° (kJ/mol)	Δ*H*° (kJ/mol)	Δ*S*° (J/mol K)
25	0.815	16.82	53.43
35	0.152		
45	-0.428		
55	-0.980		

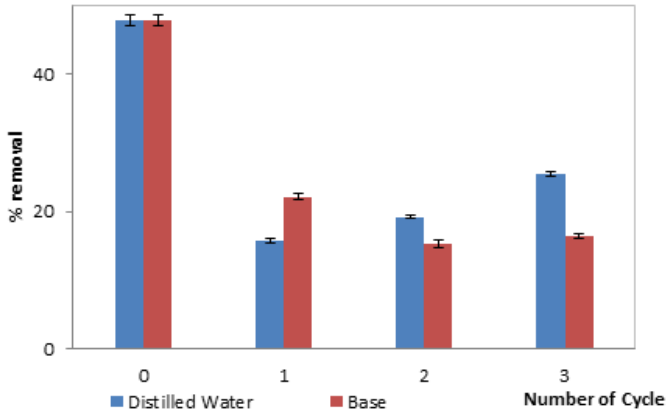

Figure 6. Regeneration experiment of JS using distilled water and 0.1 mol/L NaOH.

3.6. Regeneration experiments

To further increase the value of the adsorbent, regeneration experiments were carried out. The ability to reuse the spent adsorbent is perceived as a sustainable option. To assess the reusability, the two solvents used for regenerating the spent adsorbent were distilled water and 0.1 mol/L NaOH. The result is summarised in Figure 6. After regeneration, the % removal for spent adsorbent regenerated using distilled water and base dropped from 47.9% to 15.7% and 22.1%, respectively, and maintained about the same level on consecutive cycles. The regeneration of approximately 50% of dye adsorption capacity is perceived as reasonably high. Our previous work on the regeneration of spent Casuarina needle (Kooh et al., 2016a) and water fern (Kooh et al., 2016d) for removal of RB also reported retention of about 50% dye adsorption capacity.

4. CONCLUSIONS

This study showed the ability JS to remove RB from aqueous solution using batch adsorption method. The experiment did not require any pH alteration and the adsorption process followed the Langmuir isotherm model with maximum adsorption capacity of 26 mg/g. JS has an advantage in removing RB from water bodies as it is not severely affected by the presence of salt. Thermodynamics study indicated that the adsorption process was feasible and endothermic in nature while kinetics data showed that the pseudo-second-order model is applicable and intraparticle diffusion was not the rate limiting step. Regeneration of spent JS using water and base retained approximately 50% of the original dye removal capability after five cycles.

ACKNOWLEDGEMENTS

Appreciation is given to the Government of Brunei Darussalam and Universiti Brunei Darussalam (UBD) for their offer of Graduate Research Studies scholarship. Appreciation also goes to the Applied Physics and the Environment and Life Sciences Sections of UBD for the usage of the SEM instrument.

REFERENCES

Ahmed, T.F., Sushil, M. and Krishna, M. (2012) Impact of dye industrial effluent on physicochemical characteristics of Kshipra river, Ujjain city, India. International Research Journal of Environmental Sciences, 1, 41-45.

Anagnostopoulos, V.A., Vlachou, A. and Symeopoulos, B.D. (2015) Immobilization of *Saccharomyces cerevisiae* on low-cost lignocellulosic substrate for the removal of Cd^{2+} from aquatic systems. Journal of Environment and Biotechnology Research, 1, 23-29.

Awomeso, J.A., Taiwo, A.M., Gbadebo, A.M. and Adenowo, J.A. (2010) Studies on the pollution of water body by textile industry effluents in Lagos, Nigeria. Journal of Applied Sciences in Environmental Sanitation, 5, 353-359.

Bello, O., Inyinbor, A., Dada, A. and Oluyori, A. (2013) Impact of Nigerian textile industry on economy and environment: a Review. International Journal of Basic & Applied Sciences 13, 98-106.

Blackburn, R.S. (2004) Natural polysaccharides and their interactions with dye molecules: applications in effluent treatment. Environmental science & technology, 38, 4905-4909.

Chieng, H.I., Lim, L.B.L. and Priyantha, N. (2015) Sorption characteristics of peat from Brunei Darussalam for the removal of rhodamine B dye from aqueous solution: adsorption isotherms, thermodynamics, kinetics and regeneration studies. Desalination and Water Treatment, 55, 664-677.

Chieng, H.I., Zehra, T., Lim, L.B.L., Priyantha, N. and Tennakoon, D.T.B. (2014) Sorption characteristics of peat of Brunei Darussalam IV: equilibrium, thermodynamics and kinetics of adsorption of methylene blue and malachite green dyes from aqueous solution. Environmental Earth Sciences, 72, 2263-2277.

Dahri, M.K., Kooh, M.R.R. and Lim, L.B.L. (2014) Water remediation using low cost adsorbent walnut shell for removal of malachite green: Equilibrium, kinetics, thermodynamic and regeneration studies. Journal of Environmental Chemical Engineering, 2, 1434-1444.

Dahri, M.K., Kooh, M.R.R. and Lim, L.B.L. (2015) Application of *Casuarina equisetifolia* needle for the removal of methylene blue and malachite green dyes from aqueous solution. Alexandria Engineering Journal, 54, 1253–1263.

Dubinin, M.M. and Radushkevich, L.V. (1947) Equation of the characteristic curve of activated charcoal. Proceedings of the National Academy of Sciences, 55, 327.

Foo, K.Y. and Hameed, B.H. (2010) Insights into the modeling of adsorption isotherm systems. Chemical Engineering Journal, 156, 2-10.

Forgacs, E., Cserháti, T. and Oros, G. (2004) Removal of synthetic dyes from wastewaters: a review. Environment International, 30, 953-971.

Freundlich, H.M.F. (1906) Over the adsorption in solution. Journal of Physical Chemistry, 57, 385-471.

Hameed, B.H., Din, A.T.M. and Ahmad, A.L. (2007) Adsorption of methylene blue onto bamboo-based activated carbon: kinetics and equilibrium studies. Journal of hazardous materials, 141, 819-825.

Ho, Y.S. and McKay, G. (1999) Pseudo-second order model for sorption processes. Process Biochemistry, 34, 451-465.

Hu, Y., Guo, T., Ye, X., Li, Q., Guo, M., Liu, H. and Wu, Z. (2013) Dye adsorption by resins: Effect of ionic strength on hydrophobic and electrostatic interactions. Chemical Engineering Journal, 228, 392-397.

Idowu, A.A., Sunday, O. and Olateju, K.S. (2016) Removal of Mn(II) from aqueous solution by *Irvingia gabonensis* immobilized *Aspergillus* sp. TU-GM14: Isothermal, kinetics and thermodynamic studies. Journal of Environment and Biotechnology Research, 3, 1-11.

Kant, R. (2012) Textile dyeing industry an environmental hazard. Natural Science, 4, 22-26.

Kavitha, D. (2016) Adsorptive removal of phenol by thermally modified activated carbon: Equilibrium, kinetics and thermodynamics. Journal of Environment and Biotechnology Research, 3, 24-34.

Kooh, M.R.R., Dahri, M.K. and Lim, L.B.L. (2016a) The removal of rhodamine B dye from aqueous solution using *Casuarina equisetifolia* needles as adsorbent. Cogent Environmental Science, 2, 1140553.

Kooh, M.R.R., Dahri, M.K., Lim, L.B.L. and Lim, L.H. (2015a) Batch adsorption studies on the removal of acid blue 25 from aqueous solution using *Azolla pinnata* and soya bean waste. Arabian Journal for Science and Engineering, doi: 10.1007/s13369-015-1877-5

Kooh, M.R.R., Dahri, M.K., Lim, L.B.L., Lim, L.H. and Malik, O.A. (2016b) Batch adsorption studies of the removal of methyl violet 2B by soya bean waste: isotherm, kinetics and artificial neural network modelling. Environmental Earth Sciences, 75, 1-14.

Kooh, M.R.R., Lim, L.B.L., Dahri, M.K., Lim, L.H. and Sarath Bandara, J.M.R. (2015b) *Azolla pinnata*: An efficient low cost material for removal of methyl violet 2B using adsorption method. Waste Biomass Valorization, 6, 547-559.

Kooh, M.R.R., Lim, L.B.L., Lim, L.H. and Bandara, J.M.R.S. (2016c) Batch adsorption studies on the removal of malachite green from water by chemically modified *Azolla pinnata*. Desalination and Water Treatment, 57, 14632-14646.

Kooh, M.R.R., Lim, L.B.L., Lim, L.H. and Dahri, M.K. (2016d) Separation of toxic rhodamine B from aqueous solution using an efficient low-cost material, *Azolla pinnata*, by adsorption method. Environmental Monitoring and Assessment, 188, 1-15.

Lagergren, S. (1898) Zur Theorie der Sogenannten Adsorption gel Ster Stoffe. Kongl. Svenska Vetenskaps Academiens Handlingar, 24, 1-39.

Langmuir, I. (1916) The constitution and fundamental properties of solids and liquids. Journal of the American Chemical Society, 38, 2221-2295.

Lim, L.B.L., Priyantha, N., Tennakoon, D.T.B., Chieng, H.I., Dahri, M.K. and Suklueng, M. (2014) Breadnut peel as a highly effective low-cost biosorbent for methylene blue: Equilibrium, thermodynamic and kinetic studies. Arabian Journal of Chemistry, 10.1016/j.arabjc.2013.12.018

Liu, Y. (2008) New insights into pseudo-second-order kinetic equation for adsorption. Colloids and Surfaces A: Physicochemical and Engineering Aspects, 320, 275-278.

Madruga, M.S., de Albuquerque, F.S.M., Silva, I.R.A., do Amaral, D.S., Magnani, M. and Queiroga Neto, V. (2014) Chemical, morphological and functional properties of Brazilian jackfruit (*Artocarpus heterophyllus* L.) seeds starch. Food Chemistry, 143, 440-445.

McKay, G., Blair, H.S. and Gardner, J.R. (1982) Adsorption of dyes on chitin. I. Equilibrium studies. Journal of Applied Polymer Science, 27, 3043-3057.

Olu-Owolabi, B.I., Diagboya, P.N. and Adebowale, K.O. (2014) Evaluation of pyrene sorption–desorption on tropical soils. Journal of Environmental Management, 137, 1-9.

Prakash, O., Kumar, R., Mishra, A. and Gupta, R. (2009) *Artocarpus heterophyllus* (Jackfruit): An overview. Pharmacognosy Reviews, 3, 353-358.

Rehman, M.S.U., Munir, M., Ashfaq, M., Rashid, N., Nazar, M.F., Danish, M. and Han, J.-I. (2013) Adsorption of Brilliant green dye from aqueous solution onto red clay. Chemical Engineering Journal, 228, 54-62.

Santhi, T., Prasad, A.L. and Manonmani, S. (2014) A comparative study of microwave and chemically treated *Acacia nilotica* leaf as an eco friendly adsorbent for the removal of rhodamine B dye from aqueous solution. Arabian Journal of Chemistry, 7, 494-503.

SIGMA-ALDRICH (2014) Rhodamine B [Material Safety Data Sheet] Version 5.4 http://www.sigmaaldrich.com/MSDS/MSDS/PrintMSDSAction.do?name=msdspdf_150379221603834 Accessed 21 Sep 2015.,

Sips, R. (1948) Combined form of Langmuir and Freundlich equations. Journal of Chemical Physics, 16, 490-495.

Vijayaraghavan, K. (2015) Biosorption of lanthanide (praseodymium) using *Ulva lactuca*: Mechanistic study and application of two, three, four and five parameter isotherm models. Journal of Environment and Biotechnology Research, 1, 10-17.

Wang, M.-H., Li, J. and Ho, Y.-S. (2011) Research articles published in water resources journals: A bibliometric analysis. Desalination and Water Treatment, 28, 353-365.

Weber, T.W. and Chakravorti, R.K. (1974) Pore and solid diffusion models for fixed-bed adsorbers. American Institute of Chemical Engineers Journal, 20, 228.

Weber, W. and Morris, J. (1963) Kinetics of adsorption on carbon from solution. Journal Sanitary Engeering Division Proceedings. American Society of Civil Engineers, 89, 31-60.

Zehra, T., Priyantha, N., Lim, L.B.L. and Iqbal, E. (2015) Sorption characteristics of peat of Brunei Darussalam V: removal of Congo red dye from aqueous solution by peat. Desalination and Water Treatment, 54, 2592-2600.